SCIENCE CHINA
Earth Sciences

• RESEARCH PAPER •

June 2014 Vol.57 No.6: 1212–1220
doi: 10.1007/s11430-013-4739-6

Three-dimensional *in situ* stress determination by anelastic strain recovery and its application at the Wenchuan Earthquake Fault Scientific Drilling Hole-1 (WFSD-1)

SUN DongSheng[1,2*], LIN WeiRen[3], CUI JunWen[4], WANG HongCai[1,2], CHEN QunCe[1,2], MA YinSheng[1,2] & WANG LianJie[1]

[1] *Institute of Geomechanics, Chinese Academy of Geological Sciences, Beijing 100081, China;*
[2] *Key Laboratory of Neotectonic Movement and Geohazard, Ministry of Land and Resources, Beijing 100081, China;*
[3] *Kochi Institute for Core Sample Research, Japan Agency for Marine-Earth Science and Technology (JAMSTEC), Nankoku 783-8502, Japan;*
[4] *State Key Laboratory for Continental Tectonics and Dynamics, Institute of Geology, Chinese Academy of Geological Sciences, Beijing 100037, China*

Received April 9, 2013; accepted July 26, 2013; published online December 10, 2013

In situ stress state becomes more and more significant with in-depth research on geodynamics and energy development. However, there has not been an economic and effective method developed to determine deep three-dimensional *in situ* stress. The Anelastic Strain Recovery (ASR) method is a newly developed technique that can determine three-dimensional *in situ* stresses. After the 12 May 2008 M_s8.0 Wenchuan earthquake, the ASR method was used for the first time in mainland China to measure the *in situ* stresses in the WFSD scientific boreholes in Sichuan Province, China. In this paper, the basic procedure of the ASR method is introduced in detail and the compliances of ASR for boring cores are investigated. The results show that the maximum principal stress direction was NW64° at a measured depth (MD) of 1173 m (vertical depth 1151 m) in WFSD-1. The ratio of shear mode to the volume mode compliance of ASR was 2.9. And the three principal stresses at 1173 m MD in WFSD-1 are 43, 28 and 25 MPa. Combined with stress measurement results determined using other *in situ* measurement methods along the Longmenshan fault zone, the directions of the maximum horizontal principal stress changes from E-W to NEE-SWW to NWW-SEE when moving from NE to SW along the Longmenshan fault zone. This change is in agreement with the stress regime of the Longmenshan fault zone of the Wenchuan Earthquake, which supports a stress regime consisting predominantly of thrusts in the southwest and strike-slip in the northeast.

Wenchuan earthquake, anelastic strain recovery, compliance of anelastic strain recovery, three-dimensional *in situ* stress, scientific borehole

Citation: Sun D S, Lin W R, Cui J W, et al. 2014. Three-dimensional *in situ* stress determination by anelastic strain recovery and its application at the Wenchuan Earthquake Fault Scientific Drilling Hole-1 (WFSD-1). Science China: Earth Sciences, 57: 1212−1220, doi: 10.1007/s11430-013-4739-6

For a better understanding of earthquake generation mechanisms, the dynamic processes of surface rupture and seismic cycle characteristics, a large number of scientific research projects and drilling programs have been carried out for violent earthquakes(Ma et al., 1987; Zhang, 1987; Bohnhoff et al., 2004; Hickman et al., 2004; Wu et al., 2007; Yamashita et al., 2004; Stein, 1999; Hardebeck, 2004; Lin et al., 2007a; Chester et al., 2012; Wolter et al., 1989; Hung et al., 2009). As one of the direct driving forces that induces earthquakes, *in situ* stresses are a major objective in scientific drilling projects designed to study earthquake mecha-

*Corresponding author (email: dongshengsun@189.cn)

nisms (Wang et al., 2012; Lin et al., 2011; Shi et al., 2010; Zhang et al., 2010; Chen, 2009; Brown et al., 1978; Sun et al., 2013; Chang et al., 2010). Measurements of stress in the Earth's crustal rock masses have been attempted by various direct and indirect methods (Zang et al., 2010). Based on a careful assessment of existing stress measurement methods, we have concluded that there is no perfect method to reliably determine the magnitudes and orientations of the three-dimensional (3D) *in situ* stresses at great depth (Dey et al., 1988). For deep boreholes, the most common *in situ* stress measurement methods include hydrofracturing, differential strain curve analysis, borehole breakouts and drilling to induce tensile fractures.

Anelastic strain recovery is a newly-developed oriented-core-based method to determine the *in situ* stresses of a deep borehole. This method, which has a relatively explicit theoretical basis in comparison to other core-based methods, was firstly proposed by Voight (1968) and practically applied in petroleum engineering as a two-dimensional (2D) method by Teufel (Voight, 1968; Engelder, 1984; Warpinski et al., 1989; Perreau et al., 1989). Matsuki (1991) extended the ASR method to 3D *in situ* stress measurement. Thus this method has been chosen and employed widely in scientific drilling studies on earthquakes and structures (Matsuki et al., 1993; Lin et al., 2006; Lin et al., 2007b; Byrne et al., 2009).

Compared with hydrofracturing and other downhole experiments for *in situ* stress measurements, the advantages of the ASR method are that it is simple, inexpensive and 3D, if the cost of drilling and retrieving cores is not taken into consideration. The main disadvantage of the ASR method is that it does not directly measure stress, but rather measures anelastic strain after stress release to then determine the stress. Thus, for determining 3D *in situ* stress magnitudes, the anelastic strain recovery compliances of rock are also needed. In previous research, the magnitudes of *in situ* stresses have been determined by assuming that the ratio of the shear mode to volume mode compliance is equal to 2 (Wang et al., 2012; Lin, 2008; Brereton et al., 1995).

In this paper, we shall first briefly introduce the basic principles and related procedures of the ASR method. Then we will discuss anelastic strain recovery measurements and the ASR compliance investigation of the cores conducted to estimate both the *in situ* stress orientation and magnitude at a measured depth (MD) of 1173 m (vertical depth 1151 m) in WFSD-1. Finally, combining the results from other *in situ* stress measurement methods, a change law for the maximum horizontal principal stress orientation along the Longmenshan fault zone is analyzed and the factors influencing the ASR method are discussed. It is better for *in situ* stress measurement to use a variety of methods (at least two) to improve the credibility of the results. However, the WFSD-1 cores are generally too broken up, so methods of *in situ* stress measurement other than the ASR method could not be implemented.

1 Method

1.1 Basic principles

Anelastic strain recovery of a rock core followed by elastic strain recovery occurs immediately after a rock core is retrieved from formation, i.e., the stress field. This is based on the principle that a rock is a kind of viscoelastic material with rheological properties (Jaeger et al., 1981; Yin, 1985; Chen, 1988). When loading is applied on a rock, elastic deformation happens at the same time as loading and then transient creep takes place over time under a constant stress. Once the loading is removed, the elastic deformation is recovered immediately and the anelastic strain gradually recovers over a long period (Figure 1). Voight (1968) suggested that the recovered anelastic strain was proportional to the total recoverable strain (both elastic and anelastic strains), and hence to the pre-existing state of stress in rheologically isotropic rocks. The *in situ* stresses can be estimated by the recovered anelastic strain.

1.2 Constitutive equations

For an isotropic viscoelastic material, when *in situ* stresses and pore pressure are released step-wisely at t=0, anelastic normal strain $\varepsilon_a(t)$ recovers during the elapsed time from 0 to t in an arbitrary direction. The directions of the cosines of this arbitrary direction, defined as l, m and n, corresponding to the X, Y, Z axes, are given by the following equation (Lin et al., 2006):

$$\varepsilon_a(t)=\frac{1}{3}\begin{bmatrix}(3l^2-1)\sigma_x+(3m^2-1)\sigma_y+(3n^2-1)\sigma_z\\+6lm\tau_{xy}+6mn\tau_{yz}+6nl\tau_{zx}\end{bmatrix}\times Jas(t)+(\sigma_m-p_0)Jav(t)+\alpha_T\Delta T(t), \quad (1)$$

where σ_x, σ_y, σ_z, τ_{xy}, τ_{yz}, τ_{zx} are the components of the *in situ* stress tensor released by drilling; σ_m is the constant mean normal stress, p_0 is the pore pressure, α_T is the linear thermal expansion coefficient, $\Delta T(t)$ is the temperature change, and $Jas(t)$ and $Jav(t)$ are the anelastic strain recovery compliances

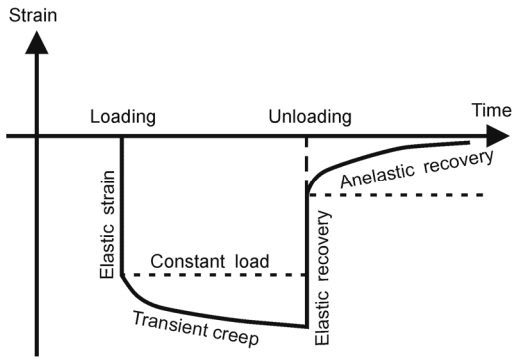

Figure 1 Schematic diagram of rock rheological property(Wang et al., 2012).

of the shear and volumetric deformation modes, respectively. The magnitudes of the three principal stresses can be simplified as follows

$$\sigma_i = e_i(t)/Jas(t) + \{e_m(t) - \alpha_T \Delta T(t)\}/Jav(t) + p_0,\ i = 1,2,3, \quad (2)$$

where $e_i(t)$ denotes the principal strain deviatoric components, and $e_m(t)$ is the constant mean normal strain.

Eq. (1) shows that the recovered anelastic strain depends on the *in situ* stress tensor components, pore pressure, temperature change during the measurement, thermal expansion coefficient and the compliances of both deformation modes. Therefore, if the material constants ($Jas(t)$, $Jav(t)$, α_T), pore pressure and temperature change are known, the six stress components, i.e., 3D *in situ* stress tensor, may be obtained by measuring the anelastic normal strains in the six independent directions. For isotropic viscoelastic materials, the directions of the three principal axes of the *in situ* stresses coincide with the directions of the three principal axes of the anelastic strain tensor. Thus, the directions of the 3D principal *in situ* stresses can be determined by means of calculating the principal directions of the measured anelastic strain data in at least six independent directions. Figure 2 shows a technical flow chart of ASR method.

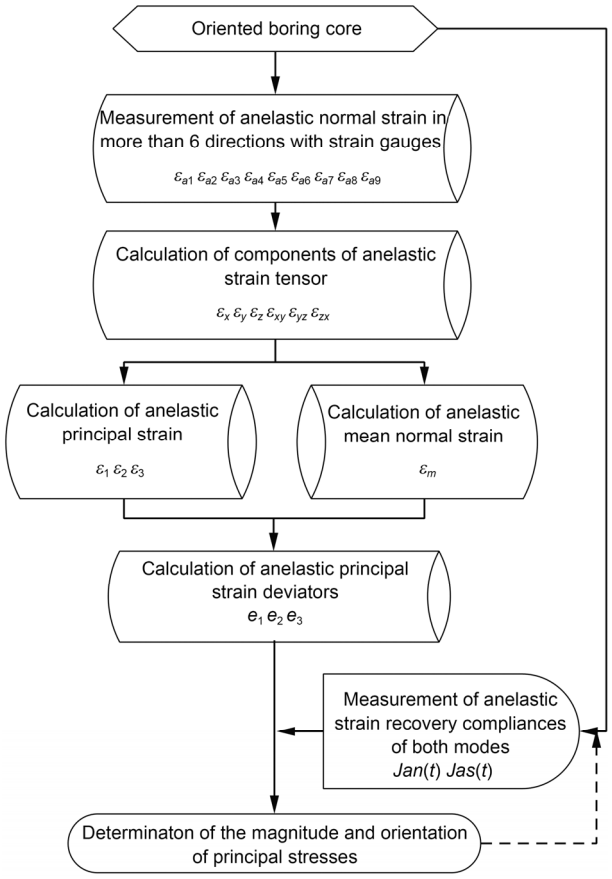

Figure 2 The procedure to determine 3-D *in situ* stresses by the ASR method (Matsuki et al., 1993).

1.3 Measurement of recovered anelastic strain

Measurements of the recovered anelastic strain in boring cores were conducted in the field laboratory of WFSD-1 (31.149°N, 103.691°E) (Li et al., 2012). The borehole is located about 90 km away from the epicenter, and about 400 m west of the Wenchuan earthquake surface rupture. The total measured depth of WFSD-1 is 1201.5 m MD (vertical depth 1179 m). Boring cores from 589.2 to 1201 m are from the Triassic Xujiahe Formation, and the lithology of the cores consists mainly of gray sandstone, dark-gray siltstone, carbon shale and coal-lines. A 70-cm-thick section of gouge is present near 590 m, representing the thickest gouge zones in all WFSD-1 cores (Li et al., 2012; Peng et al., 2011). To shorten the time interval between the stress release and the beginning of measurement, a core should be chosen near the bottom of the core that (by visual inspection) appears to be isotropic and without obvious cracks. The appropriate length of a core sample needed for an ASR test is about 10–15 cm. The cleaned core was marked with orientations, and the special strain gauges (C1, C2, C18) were glued along the baseline (X' axis) and lines that are at 45°, 90° and −45° from the baseline (with the clockwise direction being negative). The layout of strain gauges is shown in Figure 3. The sample with strain gauges was wrapped using a Fresco Bag which is sealed by silicon rubber to prevent the pore water from evaporating during the test. The sample was put in a water chamber with a constant electronically controlled temperature device. Measurement should start as quickly as possible, and in our WFSD example the time was less than 5 h from the time that the core was drilled to the start of ASR measurements. Three wire-resistance strain gauges and a precision data recorder were employed to record the strains and changes in temperature. At the same time, a dummy specimen was also employed with the same conditions to monitor the data drift.

In this paper, ASR measurements were conducted using the Feldspathic sandstone of the Upper Triassic Xujiahe Formation from WFSD-1 at a measured depth of 1173 m.

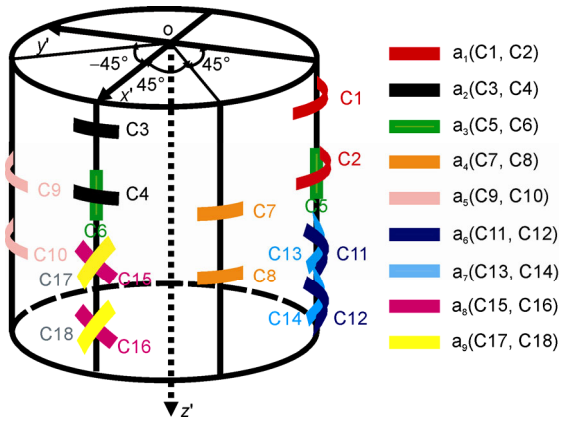

Figure 3 Layout of strain gauges on the boring core.

The results of the anelastic strain measurements for the specimen are shown in Figure 4(a). The duration of the measurement period is about one week. During the experiment, the thermostatic chamber worked properly, and the temperature of the specimen measured by a thermocouple varied by no more than ±0.1°C. In addition, the strain gauge output mounted on the dummy sandstone specimen shows that the drifts of the measurement system and the thermal expansion are so small as to be negligible.

The anelastic strains in all directions of the active specimen are extensional; all of the curves are smooth and increase similarly overtime. It is clear that the anelastic strain recovery continues in all directions for a period of more than one week, although the rate of anelastic strain recovery decreases with time. The amounts of strain in the various directions are also large enough to ensure the measurement accuracy, so these data can be used for the 3D *in situ* stresses analysis. From the measured normal strains, the anelastic strain tensor is calculated by least squares analysis, and the anelastic principal strains (ε_1, ε_2, ε_3), average strain (ε_m or e_m) and maximum differential strain (($\varepsilon_1-\varepsilon_3$)/2) are determined, as shown in Figure 4(b). The specific data process and coordinate conversion methods are adopted by the literatures (Wang et al., 2012).

1.4 Determination of the anelastic strain recovery compliances

Anelastic strain recovery compliances are inherent mechanical properties of rocks that depend on stress level and are necessary parameters for converting the anelastic strain measured on site to the three principal stresses magnitudes, a function of the anelastic strain changes caused by unit stress (Matsuki et al., 1993). The anelastic strain recovery compliances can be determined by laboratory investigations based on the basic principles of Figure 1. Matsuki (2008) conducted relative experiments to determine ASR compliances in volumetric and shear modes for seven rocks in uniaxial compression at an axial stress of 50% of the uniaxial compressive strength (UCS) to determine how much the ASR compliances depend on the rock type and to correlate the ASR compliance with conventional mechanical properties.

In this study, laboratory experiments were performed to measure ASR compliances in volumetric and shear modes using the same set of ASR measurements made on air-dried cores. The UCS was determined by UCS tests on similar rock types before the ASR experiment. The specimens were first loaded with the predetermined stress (70 MPa corresponding to 50% of its UCS) and the stress was kept constant for about 3 days. Then, the stress was relieved almost instantaneously (Figure 5(a)). And the strain recovery process was monitored for the same time as the preceding loading. The strain (both elastic and anelastic strains)-time curves are shown in Figure 5(b). During the initial period of constant compressive stress (the creep period), compressive anelastic axial strain was increased markedly; in contrast, there was a small and gradual increase of anelastic radial strain (Figure 5(c)). After unloading the compressive stress to zero, there was gradual expansion in the axial direction and contraction in the radial direction (Figure 5(c)). These deformations after unloading are known as ASR.

Figure 6 shows the anelastic strain recovery compliances of the specimen under uniaxial compression where σ_1 is 70 MPa. In this uniaxial stress condition, the magnitudes of *Jas*(*t*) and *Jav*(*t*) and the ratio of *Jas*(*t*)/*Jav*(*t*) can be determined from the following equations by measuring anelastic axial strain ε_{1a} and anelastic lateral strain ε_{3a} with strain gauges:

$$Jav(t)=\frac{\varepsilon_{1a}+2\varepsilon_{3a}}{\sigma_1+2\sigma_3},\ Jas(t)=\frac{\varepsilon_{1a}-\varepsilon_{3a}}{\sigma_1-\sigma_3}. \tag{3}$$

In some cases, the anelastic strain recovery compliances also can be determined under the experimental results of *Jas*(*t*)/*Jav*(*t*) combined with an assumption of which vertical stress is equal to the overburden pressure. Then, the anelastic

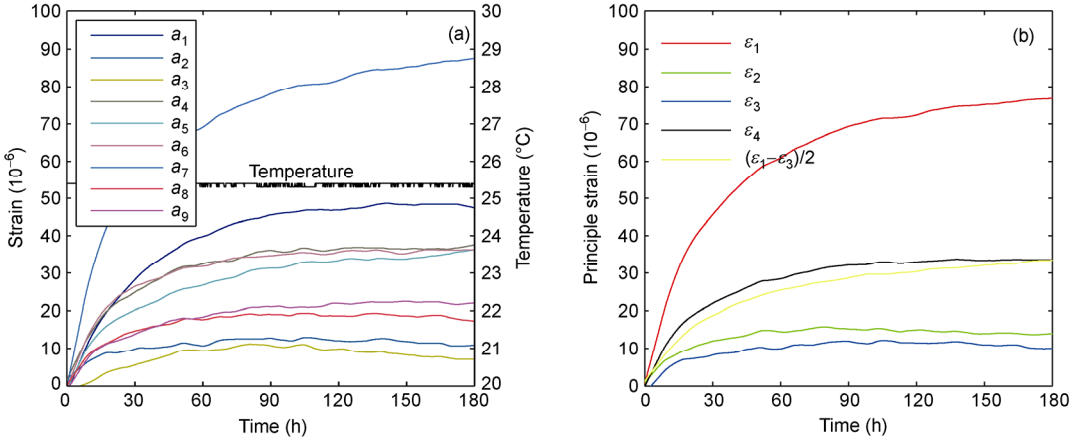

Figure 4 Curves of strain vs time. (a) anelastic recovery strains of different directions; (b) anelastic principle, average and the maximum differential strains.

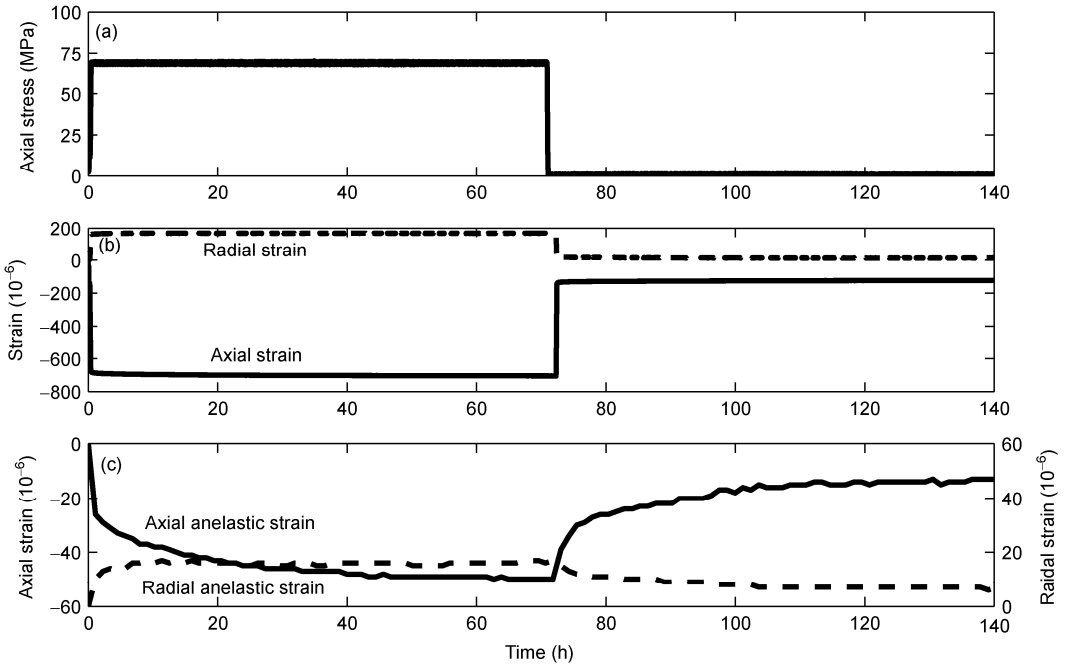

Figure 5 Determination of the anelastic strain recovery compliances. (a) Loading and unloading of axial stress; (b) total strain curves during elastic deformation, transient creep, elastic recovery and ASR; (c) anelastic strain curves during transient creep and ASR. The solid line is the axial strain and dashed line is the radial strain.

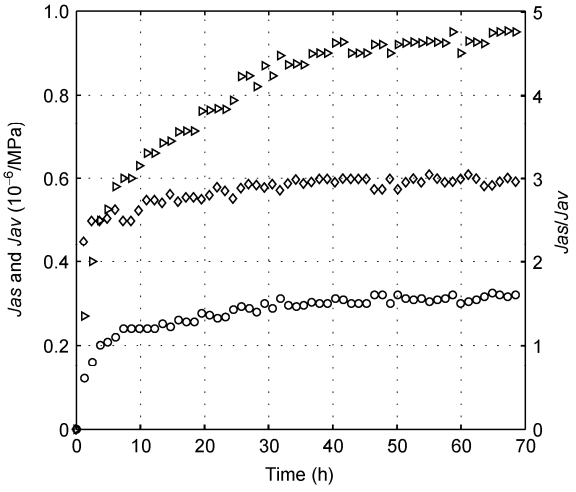

Figure 6 The anelastic strain recovery compliances calibrated in the laboratory and the ratio of $Jas(t)/Jav(t)$.

strain recovery compliances can be calculated by the following equation, and the magnitudes of the principal stresses are determined,

$$\sigma_v = \left\{\left[l_p^2 e_1(t) + m_p^2 e_2(t) + n_p^2 e_3(t)\right] \Big/ K + e_m(t)\right\} \Big/ Jav(t) + p_0, \quad (4)$$

where l_p, m_p and n_p are the directional cosines between vertical stress and the three principal axis of strain, and K is the ratio of $Jas(t)/Jav(t)$.

2 Results and analysis

2.1 *In situ* stress measurement results from WFSD-1

Anelastic strain tensors were calculated by least-squares analysis using the measured anelastic normal strains in not less than six independent directions. Then, the orientation of the three principal stresses corresponding to a particular time were determined using a data set of the three principal strains and other related deviation data for an arbitrary elapsed time. Under the assumptions that the vertical stress is the overburden pressure, and that the ratio of $Jas(t)/Jav(t)$ is about 2.9 (about 70 h after stress release) from the experimental results, the magnitude of the three principal stresses can be determined. Table 1 is the results of the

Table 1 Magnitude, azimuth and dip angle of three principal stresses

Measured depth (m)	Lithology	σ_1			σ_2			σ_3		
		Magnitude (MPa)	Azimuth (°)	Dip angle (°)	Magnitude (MPa)	Azimuth (°)	Dip angle (°)	Magnitude (MPa)	Azimuth (°)	Dip angle (°)
1173	Feldspathic sandstone	43	296	26	28	188	33	25	56	46

magnitude, azimuth and dip angle of the three principal stresses of WFSD-1 at 1173 m MD. The orientation of the maximum principal stress is NW64°. The magnitudes of the maximum, intermediate and minor principal stresses are 43, 28, and 25 MPa, respectively.

2.2 The maximum horizontal principal stress orientation along the Longmenshan fault zone

The maximum principal stress orientations at depths of 746 m (Wang et al., 2012) and 1173 m in WFSD-1 determined by the ASR method are NW49° and NW64°, respectively. These results show that the stress states lie in the reverse faulting stress regime in the footwall of the Longmenshan fault zone, which is in agreement with the features of fault slip during the M_s8.0 Wenchuan earthquake.

The orientations of the maximum principal stress in WFSD-1 determined by the ASR method are mostly consistent with the orientation of the main axes of the focal mechanism solutions of the Wenchuan earthquake and its largest aftershocks (M_s≥4.7) (Hu et al., 2008; Zheng et al., 2009; Cui et al., 2011). The principal orientations at 746 and 1173 m MD in WFSD-1 and the main axes of the focal mechanism solution for the Wenchuan earthquake are drawn in the stereogram (lower hemisphere projection) shown in Figure 7. This figure compares the principal stress orientations with those measured by ASR, hydrofracturing and structural geology analysis methods (Chen et al., 2012; Wu et al., 2009; An et al., 2004; Feng et al., 2013; Xie et al., 2004; Du et al., 2009; Liu et al., 2012). The segmentation characteristics of the maximum principal stress orientations are obtained by statistical methods (Chen et al., 2012). The dominant orientations of the maximum principal stress are E-W for northeast segment (green arrow), NEE-SWW for the mid-segment (blue arrow), and NWW-SEE for the south-west segment (black arrow) along the Longmenshan fault

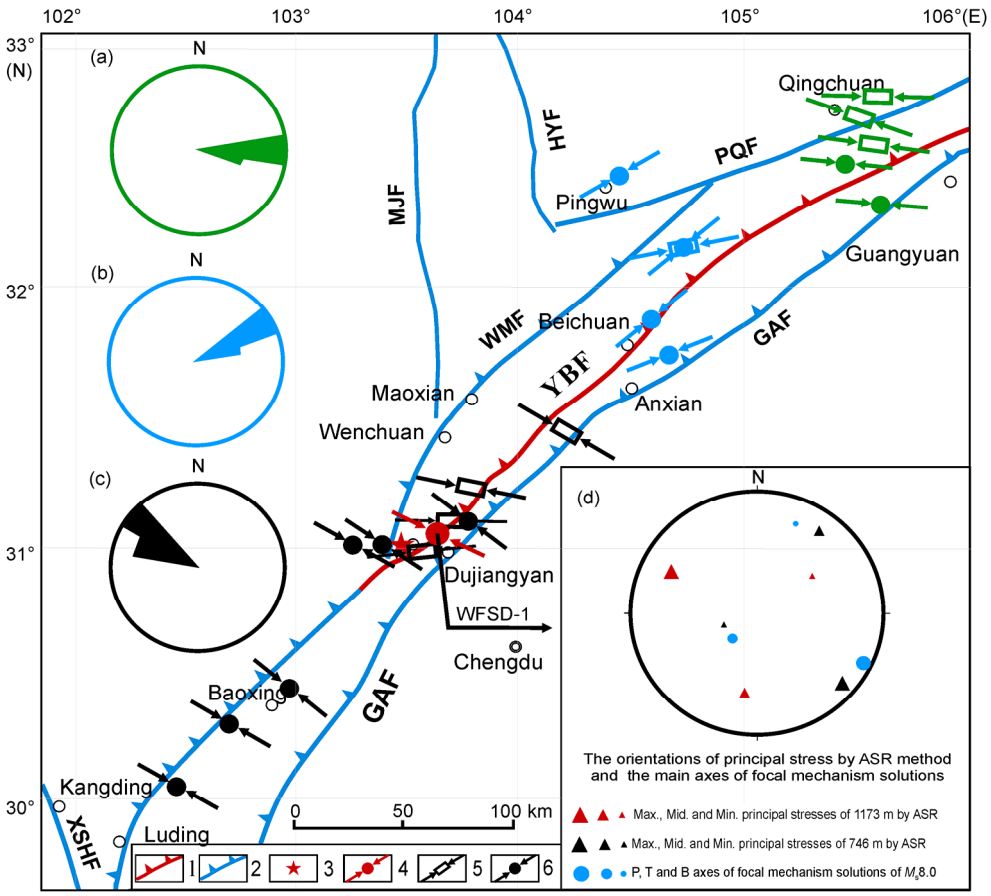

Figure 7 Tectonic map and the orientations of the maximum principal stress along the Longmenshan fault zone. WMF: Wenchuan-Maoxian fault; YBF: Yingxiu-Beichuan fault; GAF: Guanxian-Anxian fault; PQF: Pingwu-Qingchuan fault; XSHF: Xianshuihe fault; MJF: Minjiang fault; HYF: Huya fault. (a), (b) and (c) are the dominant orientations of maximum principal stress of north-east, middle and south-west segments along Longshenshan fault respectively. (d) is the stereogram results of the orientation of principal stress by ASR and the main axes of focal mechanism solution of M_s8.0 Wenchuan earthquake. 1-Seismogenic fault of 5.12 earthquake; 2-fault; 3-epicenter of 5.12 earthquake (Hu et al., 2008; Zheng et al., 2009; Cui et al., 2011); 4-WFSD-1 and the orientation of the maximum principal stress; 5-maximum horizontal principal stress orientation by the mechanisms of fault slip (Xie et al., 2004; Du et al., 2009; Liu et al., 2012); 6-maximum horizontal principal stress orientation by hydrofracturing method (Chen et al., 2012; Wu et al., 2009; An et al., 2004; Feng et al., 2013).

zone. The statistical results of the maximum principal stress orientations for the three segments are shown in Figure 7(a)–(c), which implies a change from E-W to NEE-SWW to NWW-SEE laws for the maximum principal stress orientations moving from NE to SW along Longmenshan fault zone. This is also in agreement with the change in movement characteristics from dominant thrusts in the southwest to dominant slip in the northeast along the Longmenshan fault zone.

2.3 Effects of ASR compliance on the magnitudes of *in situ* stresses

When estimating the magnitude of principal *in situ* stresses without first calibrating both the anelastic strain recovery compliances of the volumetric deformation mode and the shear deformation mode, two assumptions are normally needed. One is that the ratio of the two compliances is equal to a constant (i.e., $Jas(t)/Jav(t)$=constant) and the other is the vertical stress is equal to the overburden pressure. According to the results of this paper and Matsuki (2008), the ratio of the two compliances determined by laboratory experimental tests falls in a relatively narrow range from 1 to 3. In general, however, the ratio is not a constant, as it may be affected by such factors as lithofacies or the stress environment.

In this paper, the relationship between the estimated principal stress values and the ratio of $Jas(t)/Jav(t)$ was analyzed to examine the effect of variation in $Jas(t)/Jav(t)$ on the estimated magnitudes of the principal stresses. Figure 8 shows the simulated results on the sample from this study. From the results, a tendency for the principal stresses to decrease as the value of $Jas(t)/Jav(t)$ increases has been observed. In this case, the deviations of the maximum, intermediate and minimum principal stresses were 5.7%, 4.6% and 4.4%, respectively, if the ratio of $Jas(t)/Jav(t)$ was assumed to be equal to 2, rather than the experimental results of 2.9. In some cases, however, the maximum principal stress decreased and the intermediate and the minimum principal stress increased as the ratio of $Jas(t)/Jav(t)$ increased (Lin et al., 2006). At present, experimental results showing anelastic strain recovery compliances are limited, and much more related experimental data are needed to improve the relative accuracy of the relationship between the ratio of $Jas(t)/Jav(t)$ and the principal stresses.

2.4 Effect of time factor

Elastic and anelastic strain begin to recover as soon as *in situ* stress is relieved. However, a certain time is required to raise a rock core up from the great depth of the borehole and for surface pretreatment of the core for the experiment. Therefore the initial anelastic recovery strain cannot be recorded. At the same time, the anelastic recovery rate decreases with increasing time. This means that the amount of anelastic recovery strain decreases sharply with the time delay to the start of measurement, which tends to lower the test accuracy. Therefore, ASR measurements should be started as soon as possible once the rock core is brought to the surface. The time delay also should be considered during anelastic strain recovery calibration tests. Only the time of the anelastic strain recovery compliances corresponds to the anelastic recovery strain that is measured at the on-site laboratory; the magnitude of *in situ* stress then can be determined accurately.

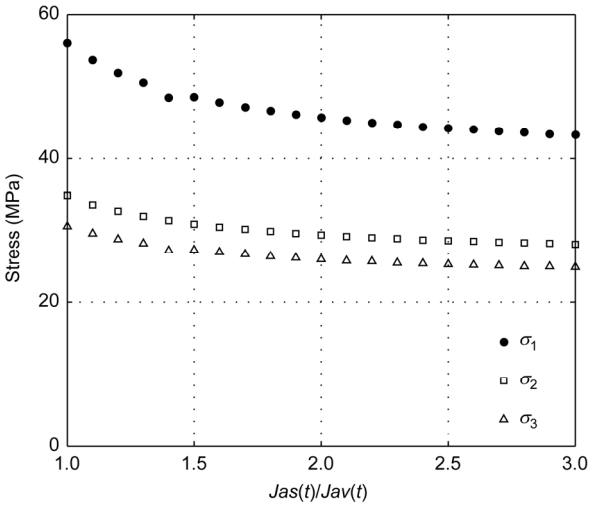

Figure 8 Estimated *in situ* stress magnitudes vs. the ratio of shear deformation mode to volumetric deformation mode compliances.

2.5 Effect of temperature changes

There is no doubt that maintaining a constant temperature is of utmost importance during the anelastic recovery strain measurement process. In general, the accuracy of *in situ* stress estimations cannot be ensured by using the apparent anelastic strain that contains some deformation due to thermal expansion. For cases where the thermal properties of rock material are isotropic, thermal expansion will only affect the mean strain and will have no effect on the strain deviation tensor. As mentioned above, the directions of the principal stresses are equal to those of the principal strain deviations; so the temperature change has no influence on the direction of principal stresses. However, the magnitudes of the principal stresses are calculated from the absolute values of recovered anelastic strain and two anelastic strain recovery compliances, so the temperature change influences the magnitudes of the principal *in situ* stresses. In this paper, temperature is controlled by the water bath controller with a fluctuation accuracy of ±0.1°C. At the same time, the influence of temperature on wire resistance is eliminated by used the three-wire strain gauges.

For the anelastic strain recovery compliances tests in the laboratory, an air-conditioning system was used to eliminate the temperature difference between day and night, but the

effect of the temperature control was not particularly good. So, a dummy sample was used to correct strain values in all directions by subtracting the same dummy strain that induced by temperature change.

2.6 Analysis of other influencing factors

The prerequisites of the ASR *in situ* stress measurement method are that the medium is homogeneous and isotropic. To ensure the reliability of the results, specific sections of homogeneous and isotropic rock core are chosen for ASR measurements. At the same time, the *in situ* state of cores was preserved as much as possible using a sealed aluminum foil bag to avoid the influence of moisture change. For the ASR method, the greater the depth of the cores, the better, as the *in situ* stress at greater depth is generally bigger and therefore the recovered anelastic strain is greater too. The strength of cores also has a certain influence on the amount of recovered anelastic strain; for example, in hard rock environments, deep cores are more necessary (Zang et al., 2010).

3 Conclusions

In this paper, the ASR method has been employed to measure *in situ* stresses in the WFSD-1 borehole, and obtain 3D recovered anelastic strain determinations at a measured depth of 1173 m. At the same time, calibration tests of the anelastic strain recovery compliances for the same core were conducted, and the magnitudes of the principal stresses were determined. The maximum, intermediate and minimum principal stresses are 43, 28 and 25 MPa, respectively. These results determined by the ASR method are basically consistent with those made by other methods.

Combining the principal stress measurement results with those determined using other *in situ* measurement methods along the Longmenshan fault zone, the principal stresses follow an orientation law that changes from E-W to NEE-SWW to NWW-SEE moving from NE to SW along the Longmenshan fault zone, which agrees with the stress regime of the Longmenshan fault zone known from the Wenchuan Earthquake to be predominantly thrust oriented in the southwest and strike-slip in the northeast.

The ASR method can be applied to achieve more reliable data when stress relief and hydraulic fracturing methods cannot be applied in complicated geological conditions, such as those that occur at great depths, high temperatures, and in boreholes with cracked strata. Therefore, it can be said that the ASR method is well suited for more complicated environments and has a wide applicability. At the same time, the calibration of the anelastic strain recovery compliances is necessary, which can improve the accuracy and reliability of *in situ* stress magnitudes determined by the ASR method.

We gratefully acknowledge three anonymous reviewers for their careful reading and constructive comments which helped us to improve this manuscript. This research was financially supported by the "Wenchuan Earthquake Fault Scientific Drilling" of the National Science and Technology Planning Project, Sinoprobe Deep Exploration in China Project (Grant No. SinoProbe-07), Fundamental Research Fund for Chinese Academy of Geological Sciences (Grant No. SYS1301), Grant-in-Aid for Scientific Research of Japan Society for the Promotion of Science (JSPS) (Grant No. 25287134) and Ministry of Education, Culture, Sports, Science and Technology (MEXT), Japan (Grant No. 21107006).

An Q M, Ding L F, Wang H Z, et al. 2004. Research of property and activity of Longmen Mountain fault zone (in Chinese). Crustal Deform Earthq, 24: 115–119

Bohnhoff M, Baisch S, Harjes H P. 2004. Fault mechanisms of induced seismicity at the super deep German Continental Deep Drilling Program (KTB) borehole and their relation to fault structure and stress field. J Geophy Res, 109: B02309, doi: 10.1029/2003JB002528

Brereton N R, Chroston P N, Evans C J. 1995. Pore pressure as an explanation of complex anelastic strain recovery results. Rock Mech Rock Eng, 28: 59–66

Brown E T, Hoek E. 1978. Trends in relationships between measured rock *in situ* stresses and depth. Int J Rock Mech Min Sci Geomech Abstr, 15: 211–215

Byrne T B, Lin W, Tsutsumi A, et al. 2009. Anelastic strain recovery reveals extension across SW Japan subduction zone. Geophys Res Lett, 36: L23310, doi: 10.1029/2009GL040749

Chang C, McNeill L C, Moore J C, et al. 2010. *In situ* stress state in the Nankai accretionary wedge estimated from borehole wall failures. Geochem Geophys Geosyst, 11: Q0AD04, doi: 10.1029/2010GC003261

Chen Q C, Feng C J, Meng W, et al. 2012. Analysis of *in situ* stress measurements at the northeastern section of the Longmenshan fault zone after the 5·12 Wenchuan earthquake (in Chinese). Chin J Geophys, 55: 3923–3932

Chen Y. 1988. Mechanical Properties of Crest Rock: Theoretical Foundation and Experimental Methods (in Chinese). Beijing: Seismological Press. 279

Chen Y. 2009. Is the Wenchuan Earthquake induced by Zipingpu reservoir? Sci China Ser D-Earth Sci, 52: 431–433

Chester F M, Mori J J, Toczko S, et al. 2012. Japan Trench Fast Drilling Project (JFAST). IODP Prel Rept, 343/343T. doi: 10.2204/iodp.pr.343343T.2012

Cui X F, Hu X P, Yu C Q, et al. 2011. Research on focal mechanism solutions of Wenchuan earthquake sequence (in Chinese). Acta Sci Nat Univer Pek, 47: 1063–1072

Dey T N, Kranz R L. 1988. State of stress and relationship of mechanical properties to hydrothermal alteration at Valles Caldera Core Hole 1, New Mexico. J Geophy Res, 93: 6108–6112

Du Y, Xie F R, Zhang X L, et al. 2009. The mechanics of fault slip of M_s8.0 Wenchuan earthquake (in Chinese). Chin J Geophys, 52: 464–473

Engelder T. 1984. The time-dependent strain relaxation of Algerie granite. Int J Rock Mech Min Sci Geomech Abstr, 21: 63–73

Feng C J, Chen Q C, Tan C X, et al. 2013. A preliminary study of the influence of Wenchuan M_s8.0 earthquake on *in situ* stress state near longmenshan fault zone: A case study in Beichuan and Jiangyou areas (in Chinese). Acta Seis Sin, 35: 137–150

Hardebeck J L. 2004. Stress triggering and earthquake probability estimates. J Geophys Res, 109: B04310, doi: 10.1029/2003JB002437

Hickman S, Zoback M. 2004. Stress orientations and magnitudes in the SAFOD pilot hole. Geophy Res Lett, 31: L15S12, doi: 10.1029/2004GL020043

Hu X P, Yu C Q, Tao K, et al. 2008. Focal mechanism solutions of Wenchuan earthquake and its strong aftershocks obtained from initial P wave polarity analysis. Chin J Geophys, 51: 1711–1718

Hung J H, Ma K F, Wang C Y, et al. 2009. Subsurface structure, physical properties, fault zone characteristics and stress state in the scientific drill holes of Taiwan Chelungpu Fault Drilling Project. Tectonophysics, 466: 307–321

Jaeger J C, Cook N G W. 1981. Fundamentals of Rock Mechanics. Institute of Engineering Mechanics, Chinese Academy of Sciences (Translated). Beijing: Seismological Press. 382–397

Li H, Wang H, Xu Z, et al. 2012. Characteristics of the fault-related rocks, fault zones and the principal slip zone in the Wenchuan Earthquake Fault Scientific Drilling Project Hole-1 (WFSD-1). Tectonophysics, doi: dx.doi.org/10.1016/j.tecto.2012.08.021

Lin W, Doan M L, Moore J C, et al. 2010. Present-day principal horizontal stress orientations in the Kumano forearc basin of the southwest Japan subduction zone determined from IODP NanTroSEIZE drilling Site C0009. Geophys Res Lett, 37: L13303, doi: 10.1029/2010GL043158

Lin W, Kwasniewski M, Imamura T, et al. 2006. Determination of three-dimensional *in situ* stresses from anelastic strain recovery measurement of cores at great depth. Tectonophysics, 426: 221–238

Lin W, Saito S, Yamamoto Y, et al. 2011. Principal horizontal stress orientations prior to the 2011 M_w9.0 Tohoku-Oki, Japan, earthquake in its source area. Geophy Res Lett, 38: L00G10, doi: 10.1029/2011GL049097

Lin W, Yeh E C, Ito H, et al. 2007a. Current stress state and principal stress rotations in the vicinity of the Chelungpu Fault induced by the 1999 Chi-Chi, Taiwan, Earthquake. Geophys Res Lett, 34: L16307, doi: 10.1029/2007GL030515

Lin W, Yeh E, Ito H, et al. 2007b. Preliminary results of stress measurement by using drill cores of TCDP Hole-A: An application of anelastic strain recovery method to three-dimensional *in situ* stress determination. Ter Atmos Ocea Sci, 18: 379–393

Lin W. 2008. A core-based method to determined three-dimensional *in situ* stress in deep drilling wells: anelastic strain recovery technique. Chin J Rock Mech Eng, 27: 2387–2394

Liu J, Xiong T Y, Zhao Y, et al. 2012. Kinematic characteristics of Longmenshan active fault zone and its tectonic implication. J Jilin Univer (Earth Sci Ed), 42(Suppl): 320–330

Ma Z J, Jiang M. 1987. Strong earthquake periods and episodes in China. Earthq Res China, 3: 47–51

Matsuki K, Takeuchi K. 1993. Three-dimensional *in situ* stress determination by anelastic strain recovery of a rock core. Int J Rock Mech Min Sci Geomech Abstr, 30: 1019–1022

Matsuki K. 1991. Three-dimensional *in Situ* stress measurement with anelastic strain recovery of a rock core. In: Wittke W, ed. Proc 7th Int Congr Rock Mech. Aachen. 557–560

Matsuki K. 2008. Anelastic strain recovery compliance of rocks and its application to *in situ* stress measurement. Int J Rock Mech Min Sci, 45: 952–965

Peng H, Ma X M, Jiang J J. 2011. *In situ* stress measurement by differential strain analysis method in WFSD-1 (in Chinese). J Geomechan, 17: 249–261

Perreau P J, Heugas O, Santarelli F J. 1989. Tests of ASR, DSCA, and core discing analyses to evaluate *in situ* stresses. SPE paper 17960, SPE Middle East Oil Technical Conference and Exhibition Manama, Bahrain. 325–336

Shi Y L, Cao J L. 2010. Some aspects in static stress change calculation-case study on Wenchuan earthquake. Chin J Geophys, 53: 102–110

Stein R S. 1999. The role of stress transfer in earthquake occurrence. Nature, 402: 605–609

Sun D S, Wang L J, Wang H C, et al. 2013. Analysis of the Wenchuan M_s8.0 earthquake co-seismic stress and displacement change by using the finite element method. Acta Geol Sin, 87: 1120-1128

Voight B. 1968. Determination of the virgin state of stress in the vicinity of a borehole from measurements of a partial anelastic strain tensor in drill cores. Felsmechanik und Ingenieurgeologie, 6: 201–215

Wang L J, Sun D S, Lin W R, et al. 2012. Anelastic strain recovery method to determine *in situ* stress and application example. Chin J Geophys, 55: 1674–1681

Warpinski N R, Teufel L W. 1989. *In situ* stresses in low permeability, nonmarine rocks. J Pet Tech, 41: 405–414

Wolter K E, Berckhemer H. 1989. Time dependent strain recovery of cores from the KTB-Deep drill hole. Rock Mech Rock Eng, 22: 273–287

Wu H Y, Ma K F, Zoback M, et al. 2007. Stress orientations of Taiwan Chelungpu-Fault Drilling Project (TCDP) hole-A as observed from geophysical logs. Geophy Res Lett, 34: L01303, doi: 10.1029/2006GL028050

Wu M L, Zhang Y Q, Liao C T, et al. 2009. Preliminary results of *in situ* stress measurements along the Longmenshan Fault Zone after the Wenchuan M_s8.0 eratherquare. Acta Geol Sin, 83: 746–753

Xie F R, Cui X F, Zhao J T, et al. 2004. Regional division of the recent tectonic stress field in China and adjacent areas (in Chinese). Chin J Geophys, 47: 654–662

Yamashita F, Fukuyama E, Omura K. 2004. Estimation of fault strength: Reconstruction of stress before the 1995 Kobe earthquake. Science, 306: 261–263

Yin X H. 1985. Solid Mechanics (in Chinese). Beijing: Earthquake Press. 512

Zang A, Stephansson O. 2010. Stress Field of the Earth's Crust. London: Springer. 115–193

Zhang B, Shi Y L. 2010. A discussion on the influences of Zipingpu reservoir on the stability of faults in the neighborhood. J Graduate School Chin Acad Sci, 27: 755–762

Zhang G M. 1987. Rhythmic characteristics of high seismic activity in China mainland. Seismol Geol, 9: 27–38

Zheng Y, Ma H S, Lǔ J, et al. 2009. Source mechanism of strong aftershocks (M_s≥5.6) of the 2008/05/12 Wenchuan earthquake and the implication for seismotectonics. Sci China Ser D-Earth Sci, 52: 739–753